Theoretical model used in the SOLPIC software

A. Husakou[1], O. Fedotova[2], R. Rusetsky[2], T. Smirnova[3], O. Khasanov[2], A. Fedotov[3], U. Sapaev[4]

[1]Max Born Institute, Max Born Str. 2a, D-12489 Berlin, Germany

[2]Scientific-Practical Materials Research Centre of National Academy of Sciences of Belarus, P.Brovki str. 19, 220072 Minsk, Belarus

[3]Belarus State University, Niezaliežnasci ave 4, 220030 Minsk, Belarus

[4]Tashkent State Technical University, University street 2, 100097 Tashkent, Uzbekistan

gusakov@mbi-berlin.de

Abstract. *The theoretical model which is used for developing the SOLPIC software is described. Formalism for the various physical mechanisms, such as photoionization, plasma dynamics, chromatic dispersion, second- and third-order optical nonlinearities, as well as excitonic multilevel system, is presented. Results for an exemplary simulation are shown and discussed.*

1. Introduction

We consider a composite which consists of two components: homogeneous host material and inclusions represented by randomly-distributed spherical nanoparticles. We consider a situation when the filling fraction of the inclusions is sufficiently low (typically few percent or below) so that neither percolations nor interaction between the nanoparticles play any role. Furthermore, we consider nanoparticles to be sufficiently small, so that their diameter is below the incident light wavelength in both host and inclusion materials. Note that we do not place any limitations on the nature of host and inclusion materials, i.e., either of them could be dielectric, metals, or semiconductor. We consider the inclusions to consist of a homogeneous material, however, we do not require point symmetry in either host material or in the inclusions. Due to this, the second-order susceptibility can be non-zero in either material.

The physical situation to be modelled by SOLPIC is the propagation of a relatively-short (sub-ps) pulse in such a composite. Typically, pulses in visible, near-UV or IR ranges are considered. SOLPIC is limited to (1+1)D simulation, so that the incident pulse represents a plane wave propagating through the composite. Furthermore, unidirectional propagation without significant excitation of the backward-propagating wave is considered. Regarding the intensity of the incident light, its upper limit is determined by the absence of damage and the associated back-reflection, to the values (for most materials) of 50 TW/cm^2 and below.

Under these conditions, we need to include the following effects into account: photoionization, plasma dynamics, chromatic dispersion, as well as second- and third-order optical nonlinearities. In addition, transitions between excitonic states can play a significant role in the nanoparticle response, in particular for the generation of new frequencies in the THz range. Therefore transitions between the excitonic levels are included

as well in the framework of Bloch equations. Among the effects which were neglected in this treatment we list among others thermal effects, coupling to phonons and nanoparticle deformation, Raman scattering, anisotropy of the host material, deviations of the nanoparticle form from the spherical one, and generation of high-order harmonics.

This description is organized as follows: in the Section 2, the propagation equation and methods for solving this equation are discussed. In Section 3, various contributions to the polarization are described. In Section 4, we exemplify the simulation by SOLPIC by considering a particular sample case of propagation in silica composite with ZnO inclusions. Finally, we draw conclusions in Section 5.

2. Propagation equation

If the backward reflection can be neglected, the following propagation equation can be used to model the light propagation in a homogeneous medium [1, 2], which includes linear (chromatic) group velocity dispersion and loss as well as nonlinear effects:

$$\frac{\partial E(z,\omega)}{\partial z^2} = -i\left(\frac{[\sqrt{\epsilon(\omega)}-n_g]\omega}{c} - \beta(\omega_0)\right)E(z,\omega) - \frac{i\omega}{2c\sqrt{\epsilon(\omega)}}P_{NL}(z,\omega), \quad (1)$$

where $E(z,\omega) = \hat{F}E(z,t) = \int_{-\infty}^{\infty} E(z,t)\exp(-i\omega t)dt$ is the Fourier transform $\hat{F}$ of the electric field $E(z,t)$, z is the propagation coordinate, n_g is the refractive index, ω_0 is a characteristic frequency of the pulse spectrum, $n(\omega)$ is the refractive index, and $P_{NL}(z,\omega)$ is the Fourier transform of the nonlinear part of the polarization. We would like to empathise that in our treatment no slowly-varying envelope approximation is used, and $E(z,t)$ represents the real-values field including the carrier oscillations. Such a treatment allows us to create a unified treatment for a pulse with arbitrary spectral contents. Note, however, that Fourier-transforms $E(z,\omega)$ and $P(z,\omega)$ are, generally-speaking, complex-valued.

For a rarefied composite with small inclusions as discussed above, the homogeneous-medium description provided by Eq. (1) can still be used if one substitutes the composite material by a homogenised medium in the framework of the so-called effective-medium theory. The effective-medium theory provides the following formalism for the effective dielectric function of a composite[2]:

$$\epsilon_{eff} = (1-f)\epsilon_h + f\epsilon_i\frac{3\epsilon_h}{2\epsilon_h+\epsilon_i}, \quad (2)$$

where f is the volume filling factor of the inclusions and $\epsilon_{h,i}$ are the dielectric functions of the host and of the inclusions, correspondingly. The second- and third-order susceptibilities, as well as other nonlinear processes, can also be described in the framework of the effective-medium theory, as detailed below.

The propagation equation is solved as a boundary problem, i.e., the temporal profile which enters the composite is defined and then is propagated through composite. This approach is standard in most areas of nonlinear optics, but it should not be confused with FDTD-like schemes, which utilize initial-value approach for the electric field.

We solve the propagation equation by extended split-step method, whereby each of the contributions to the polarization is treated subsequently. This standard method allows to reduce the accumulation of numerical error. Nonlinear steps are performed using the Runge-Kutta method, the order of which can be selected between 1,2, and 4. Fixed step of the grid both in time and in the propagation coordinate is used. The appearance of numerical artifacts during the propagation is monitored by tracing the total pulse energy as well as the total energy absorbed at the boundaries of the numerical time window.

3. Contributions to polarization

The total polarization is given by

$$P(z,t) = P_{chr}(z,t) + P_{NL}(z,t) = P_{chr}(z,t) + P_{\chi^{(2)}} + P_{\chi^{(3)}} + P_{plasma} + P_{ph-abs} + P_{exc}, \quad (3)$$

where the contributions correspond to chromatic dispersion, second-order susceptibility, third-order susceptibility, plasma contribution to the dielectric function, absorption due to photoionization, and contribution from exciton polarization. Below each of these terms are discussed separately.

3.1. Chromatic polarization

The expression for the chromatic polarization is given in the frequency domain as

$$P_{chr}(z,\omega) = \frac{2c\epsilon_0}{\omega}\left(\frac{[\sqrt{\epsilon(\omega)} - n_g]\omega}{c} - \beta(\omega_0)\right) E(z,\omega). \quad (4)$$

This expression includes a term characterized by n_g which corresponds to computation in a frame moving with velocity c/n_g, so that the pulse does not leave the computational domain. For the effective dielectric function ϵ_{eff}, the expression (2) was used, with values of host and inclusion dielectric function provided by Sellmeier-type expression. Note that the linear absorption is also included in this term.

3.2. Second- and third-order perturbative optical susceptibilities

The expressions for the effective second-order susceptibility look like [3]

$$\chi^{(2)}_{eff}(\omega_1,\omega_2,\omega_3) = (1-f)\chi^{(2)}_h + f x(\omega_1)x(\omega_2)x(\omega_3)\chi^{(2)}_i, \quad (5)$$

where $\chi^{(2)}_h$ and $\chi^{(2)}_i$ are the susceptibilities of host and inclusion materials, correspondingly. Note that we neglected the frequency dependence of the susceptibilities of host and inclusions. Quantity $x(\omega)$ is the ratio of local field inside the inclusion and the incident field:

$$x(\omega) = \frac{3\epsilon_h(\omega)}{2\epsilon_h(\omega) + \epsilon_i(\omega)}. \quad (6)$$

Here we note that in principle, due to photoionization as described below, the $\epsilon_i(\omega)$ and therefore x, strictly speaking, depend on time due to buildup of plasma during the pulse. However, in the framework of these simulation we neglect this dependence, assuming that corresponding relative change of $\epsilon_i(\omega)$ is much less than unity and that we are far from the plasmonic resonance given by $2\epsilon_h(\omega) = -\epsilon_i(\omega)$.

Similarly, for the effective third-order susceptibility one can derive

$$\chi^{(3)}_{eff}(\omega_1, \omega_2, \omega_3, \omega_4) = (1-f)\chi^{(3)}_h + f x(\omega_1)x(\omega_2)x(\omega_3)x(\omega_4)\chi^{(3)}_i. \tag{7}$$

The final expressions which was used to calculate the corresponding polarizations look like

$$P_{\chi^{(2)}}(z,\omega) = (1-f)\epsilon_0\chi^{(2)}_h\hat{F}E(z,t)^2 + f\epsilon_0\chi^{(2)}_i\hat{F}[\hat{F}^{-1}\{E(z,\omega)x(\omega)\}]^2 \tag{8}$$

$$P_{\chi^{(3)}}(z,\omega) = (1-f)\epsilon_0\chi^{(3)}_h\hat{F}E(z,t)^3 + f\epsilon_0\chi^{(3)}_i\hat{F}[\hat{F}^{-1}\{E(z,\omega)x(\omega)\}]^3 \tag{9}$$

3.3. Plasma contribution to the refractive index

In the framework of SOLPIC, we consider a case when the ionization potential I_p of the inclusions is low than that of the host material. In this case, the ionization rate is higher in inclusions, and due to the sensitive dependence of the polarization rate on the ionization potential, we can neglect plasma formation in host material. Although a composite is a solid material, we treat the ionization and subsequent electron motion using the paradigms typical for gases. This is justified for solid-state materials with negligible strong anharmonicity of the bands in the low-momentum region of the Brillouin zone.

The contribution from the plasma is determined by the average displacement $\langle d\rangle$ of the electron from the parent molecule, whereby by a "molecule" we consider an atom or a group of atoms of the solid-state material for which the ionization rate formalism is defined. Furthermore, it is determined by relative ionization of the solid state ρ, which is the ratio of the free-electron density to the density of molecules:

$$P_{plasma}(z,\omega) = N_{mol}e\hat{F}[\langle d\rangle(z,t)\rho(z,t)]. \tag{10}$$

Here N_{mol} is the concentration of the molecules and e is the electron charge. The above expression would be valid in a homogeneous medium; however, as it refers to a polarization which occurs inside of nanoparticles, in the case of effective-medium theory it has to be additionally multiplied by $x(\omega)$. For the origin of this factor and further details see Ref. [3].

The dynamics of the $\langle d\rangle(z,t)\rho(z,t)$ is given by [6]

$$\frac{\partial(\langle d\rangle(z,t)\rho(z,t))}{\partial t} = \langle v\rangle(z,t), \tag{11}$$

where $\langle v \rangle$ is the average velocity of electrons, and the dynamics of the $\langle v \rangle(z,t)\rho(z,t)$ is given by second Newton's law by

$$\frac{\partial(\langle d \rangle(z,t)\rho(z,t))}{\partial t} = -\frac{eE(z,t)}{m_e}\rho, \tag{12}$$

where m_e is the electron mass. Here we neglect the initial displacement and velocity of electron just after the ionization.

The dynamics of the relative plasma density ρ is given by

$$\frac{\partial \rho}{\partial t} = \Gamma(\hat{F}^{-1}[x(\omega)E(z,\omega)]), \tag{13}$$

where $x(\omega)E(z,\omega)$ is the local field inside of inclusions which determine the photoionization rate.

Depending on the relation between the frequency of pump light and the ionization potential of inclusions, we consider two models for the ionization rate. For the case when the energy of pump photons is much smaller than the ionization potential, the photoionization occurs either by multiphoton regime or by tunneling regime, as determined by intensity and Keldysh parameter. Here we utilize so-called Yudin-Ivanov model[4], which provides a formalism for both of these regimes in a unified way.

The cycle-resolved ionization rate Γ is given by (in atomic units, that is, with frequency ω, time t and field $\mathcal{E}$ measured in the corresponding Hartree units $\omega_a = 0.26$ rad/as, $t_a = 24.2$ as, $x_a = 0.0529$ nm, and $\mathcal{E}_a = 514.2$ V/nm):

$$\Gamma(z,t) = \frac{\pi}{\tau_T}\exp\left(-\sigma_0\frac{\langle 2\mathcal{E}(z,t)^2\rangle}{\omega^3}\right)\left[\frac{2\kappa^3}{\sqrt{\langle 2\mathcal{E}(z,t)^2\rangle}}\right]^{2Z/\kappa}\exp\left[-\frac{\mathcal{E}(z,t)^2}{2\omega^3}\sigma_1\right]. \tag{14}$$

Here Z is the effective atomic charge, $\kappa = \sqrt{I_p/(\hbar\omega_a)}$, $\sigma_0 = \frac{1}{2}(\gamma^2 + \frac{1}{2})\ln C - \frac{1}{2}\gamma\sqrt{1+\gamma^2}$, $C = 1 + 2\gamma\sqrt{1+\gamma^2} + 2\gamma^2$, and $\sigma_1 = \ln C$-$2\gamma/\sqrt{1+\gamma^2}$. The quantity $\langle E(z,t)^2\rangle$ is the averaged value of the squared electric field over few past periods (5 periods is assumed in this work).

For the case when the energy of pump photons is around two ionization potentials, one can use the two-photon formalism[5] and write the cycle-resolved ionization rate Γ (in SI units) as

$$\Gamma(z,t) = \frac{2e^4x_a^4\nu}{\hbar^4\omega_0^2[(2\omega_0 - I_p/\hbar)^2 + \nu^2}\langle E(z,t)^2\rangle E(z,t)^2, \tag{15}$$

where ν is the relaxation constant of the two-photon transition.

3.4. Absorption related to photoionization

The energy required for the photoionization is taken from the electric field of the pulse, causing time-dependent absorption. The corresponding loss for the electric field is given by [7]

$$\alpha(z,t) = -\frac{\Gamma(z,t)N_0 I_p e f}{2\epsilon_0 c n_g^2 E(z.t)^2}. \tag{16}$$

3.5. Excitonic contribution to polarization

We consider the excitonic levels as a multilevel system and utilize the standard Bloch equations for the description of the ionization. The dynamics of the density matrix ρ_e is given by (see e.g. [5])

$$i\hbar\frac{\partial\rho_e}{\partial t} = [H, \rho_e], \tag{17}$$

where $H = H_0 + H_{int}$, H_0 is the Hamiltonian of the system in the absence of excitation, H_{int} is the interaction Hamiltonian, which components H_{ij} are related with the corresponding dipole transition moments eM_{ij}: $H_{ij} = eM_{ij}\hat{F}^{-1}[E(z,\omega)x(\omega)]$. In addition, polarization decay (decay of the off-diagonal elements of ρ_e) with decay time T_2 and decay of the population to the ground state with decay time T_1 are included.

The excitonic polarization is then defined in a standard way as

$$P_{exc}(z,\omega) = x(\omega)\hat{F}[fTr(\rho_e M)]. \tag{18}$$

4. Sample calculation

In order to exemplify the above model and functioning of SOLPIC, we present in this section a simulation of THz generation. Note that the input parameters were not fully optimized for the THz generation efficiency, and some of the parameters are more or less accurate estimates and not precise values.

We consider a propagation of two 0.055 TW/cm^2, 15-fs (FWHM) pulses at central circular frequencies of 2.26 fs^{-1} and 2.40 fs^{-1}. Pulses propagate through a composite which consist of silica host and ZnO inclusions. Inclusions are spheres with a diameter of 3μm and volume filling factor of 0.01. For the description of the photoionization, the ionization potential of 3.37 eV was used. The chromatic dispersion was described using analytical Sellmeier-type expression for both silica and ZnO. Excitonic contribution was described using the hydrogen-type level structure, with energy levels scaled by the ration of the ionization potentials of ZnO and hydrogen, and polarization and population relaxation times of 200 fs and 400 fs correspondingly. Dipole moment were assumed to be 1 unit of atomic units (1.6×10^{-28} C·m). The following values were used for the description of the optical nonlinearities: $\chi_i^{(2)} = 5\times10^{-12}$ m/V, $\chi_h^{(2)} = 0$, $\chi_i^{(3)} = 0.33\times10^{-22}$ m^2/V^2, $\chi_h^{(3)} = 2\times10^{-22}$ m^2/V^2.

The results are presented in Fig. 1. One can see that the pump pulses do not change significantly during the propagation, however, in the spectra one can see the formation of THz part of the radiation for frequencies below $0.3\omega_0$, where ω_0 = 2.26 fs^{-1} is the central frequency of one of the input pulses. The strength of the THz radiation increases over propagation, as can be seen in Fig. 1(b), and the output efficiency of THz generation is 0.23% after 50 μm of propagation. In Fig. 1(c) we present the temporal profile of the generated THz generation. One can see that the duration of THz generation is much

longer than that of the input pulses, which is caused by the walk-off as well as by the group velocity dispersion. These effects limit the efficiency of the THz generation. In addition, we have tested the role of the excitons in the THz generation by repeating the simulation with exciton contribution switched off, and observed a very significant (by 5 orders of magnitude) decrease of the conversion efficiency, confirming the key role of the exciton dynamics.

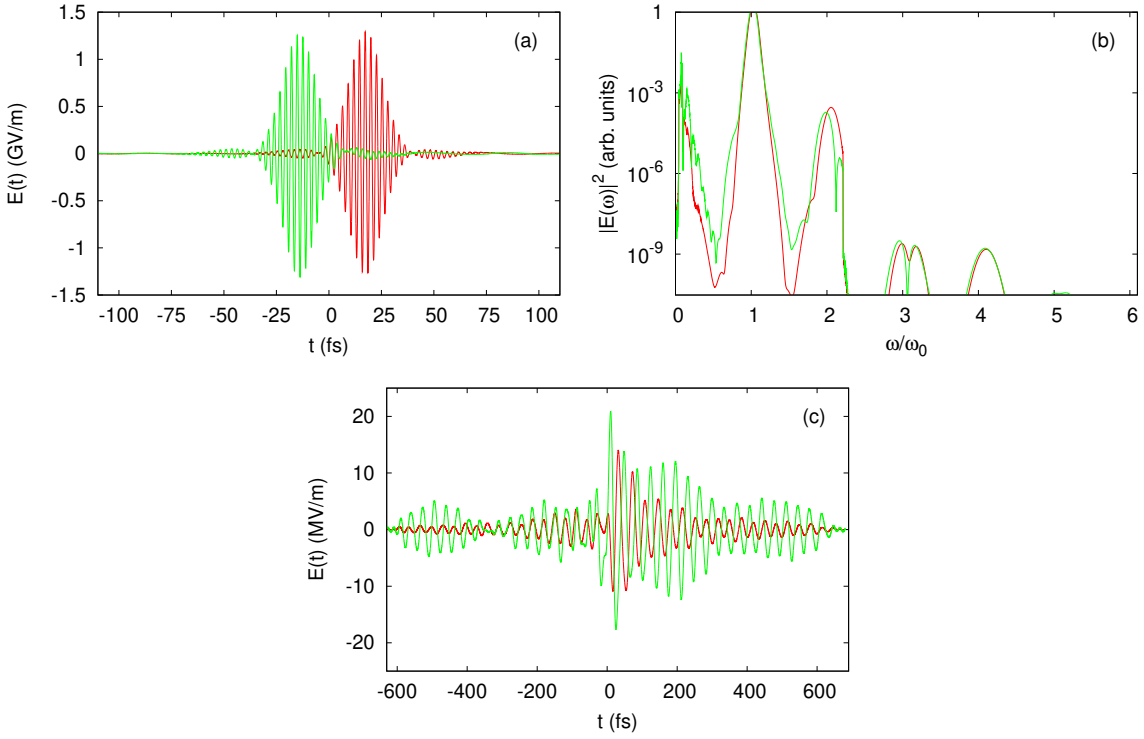

Figure 1. Temporal pulse profiles (a), spectra (b) and temporal profiles of the THz part of the pulse (c) for parameters given in text. The propagation length is 10 μm (red curves) and 50 μm (green curves).

References

[1] A. Husakou and J. Herrmann, Physical Review Letters **87** (20), 203901 (2001).

[2] J. C. Maxwell Garnett, Philos. Trans. R. Soc. London **203**, 385 (1904); **205**, 237 (1906).

[3] J. E. Sipe and R. W. Boyd, Phys. Rev. A **46**, 1614 (1992).

[4] G. L. Yudin and M. Y. Ivanov, Phys. Rev. A **64**, 013409 (2001).

[5] L. S. Meng, "Continuous-wave Raman laser in H2 : semi-classical theory and diode-pumping experiments", PhD thesis, Montana State University, 2002.

[6] A. Husakou and J. Herrmann, Opt. Express **17**, 12481 (2009).

[7] P. Jürgens *et al.*, Nat. Phys. (2020). https://doi.org/10.1038/s41567-020-0943-4